Supporting Information Appendix

Time-evolving genetic networks reveal a NAC troika that negatively regulates leaf senescence in *Arabidopsis*.

Hyo Jung Kim[a,1], Ji-Hwan Park[a,1], Jingil Kim[a], Jung Ju Kim[a], Sunghyun Hong[a], Jeongsik Kim[a], Jin Hee Kim[a], Hye Ryun Woo[b], Changbong Hyeon[c], Pyung Ok Lim[b,2], Hong Gil Nam [a,b,2] and Daehee Hwang [a,b,2]

[a]Center for Plant Aging Research, Institute for Basic Science (IBS), Daegu, 42988, Republic of Korea; [b]Department of New Biology, DGIST, Daegu, 42988, Republic of Korea; and [c]Korea Institute for Advanced Study (KIAS), Seoul, 02455, Republic of Korea.

[1]These authors contributed equally to this work.

[2]To whom correspondence should be addressed, E-mail: polim@dgist.ac.kr, nam@dgist.ac.kr, or dhwang@dgist.ac.kr

This file includes:

SI Materials and Methods

Figs. S1–8

Tables S1–3

Dataset S1–6

– Dataset S1–6 are provided in additional Excel spreadsheets.

SI Materials and Methods

NanoString nCounter assay.

Of 113 *NAC* TFs in *Arabidopsis* genome (1), 84 expressed *NAC*s in leaves were identified from the previously reported time-course RNA-sequencing data as previously described (2). Among the 84 expressed *NAC*s, we then identified 65 *NAC*s that showed temporal expression changes during leaf aging (*SI Appendix*, Fig. S1*A*). The mutant lines were available for 49 of the 65 aging-associated *NAC*s, which were used for NanoString nCounter assay. Total RNA was extracted from the *Arabidopsis* leaves using WelPrep (WelGENE) and RNA quality check to using Fragment Analyzer (Advanced Analytical Technologies). We used a custom CodeSet constructed to detect the selected *NAC*s and 18 control genes whose expression remain not altered during leaf aging. The digital multiplexed NanoString nCounter assay (NanoString Technologies) was performed with total RNA (100 ng) isolated from leaves at 4 stages (14, 18, 22, and 26 days of leaf age). Hybridizations were carried out by combining 5 ul of each RNA sample with 8 ul of nCounter Reporter probes in hybridization buffer and 2 ul of nCounter Capture probes (for a total reaction volume of 15 ul) overnight at 65℃ for 16–20 hrs. Excess probes were removed using two-step magnetic bead based purification on the nCounter Prep Station (NanoString Technologies). Abundances of specific target molecules were quantified on the nCounter Digital Analyzer by counting the individual fluorescent barcodes and assessing the target molecules. For each assay, a high-density scan encompassing 280 fields of view was performed. The data were collected using the nCounter Digital Analyzer after taking images of the immobilized fluorescent reporters in the sample cartridge with a CCD camera.

Identification of differentially expressed *NAC*s.

The count data of the samples were normalized using the previously reported normalization method for NanoString data (3). For each comparison of mutants versus wild type, target genes were determined to be expressed if their $\log_2$-count >5 in at least one of the samples in the mutant or wild type. The cutoff was determined as an integer larger than the maximum value of negative controls. We then applied the statistical method previously reported (4) to the normalized values in the time point. Briefly, for each gene, we computed T-statistic value. To estimate a false negative rate (FDR) for the T-value, we estimated an empirical null distribution of T-values as follows: 1) we randomly permuted all the samples and computed T-values for the randomly permuted samples in each time point; 2) the resulting T-values in all the time points were merged; 3) steps 1 and 2 were repeated 100,000 times; and 4) Gaussian Kernel density estimation was applied to the merged T-values to estimate an empirical distribution of T-value. For each gene, the FDR value for the observed T-value was calculated using the empirical distributions by a two-tailed test. Finally, of the expressed genes, differentially expressed *NAC*s were identified as the ones with FDR <0.1 and absolute $\log_2$-fold-change >10^{th} percentiles of the empirical distribution for $\log_2$-fold-change, which was estimated as done for T-value. The cutoffs for FDR and $\log_2$-fold-change were determined through manual validation after trying several cutoff values (0.01, 0.05, 0.1, 0.15, and 0.2).

Identification of hub NACs.

The regulatory NAC network at each stage was constructed based on the regulatory relationships among the 49 NAC TFs. To identify the hub NACs in the regulatory NAC network at each stage, the null empirical distribution of out-degree in the stage was obtained as follows: 1) the interactions in the regulatory NAC network was randomly shuffled; 2) out-degrees for 49 NACs in the randomly shuffled network were measured; 3) steps 1 and 2 were repeated 1,000 times; and 4) an empirical distribution for the out-degree was estimated by applying Gaussian kernel density estimator to the out-degrees from 1,000 random shuffling experiments. An adjusted *P* value for the observed out-degree of each NAC in the regulatory NAC network at each stage was calculated using the empirical distribution by the right-sided test. Finally, the NACs with $P < 1.0 \times 10^{-4}$ were identified as the hub NACs in the stage.

RNA isolation and qRT-PCR analysis.

Total RNA was isolated from 3rd or 4th rosette leaves using WelPrep total RNA isolation reagent (WELGENE), according to the manufacturer's instructions. First-strand cDNA was synthesized using the ImProm II Reverse Transcriptase system kit (Promega), followed by qRT-PCR analysis (Bio-Rad, CFX96 Touch Real-Time PCR Detection System). mRNA expression levels of target genes were calculated using the comparative threshold (C_T) method and normalized by those of *ACT2* (*At3g18780*). Primers used for PCR are listed in *SI Appendix*, Table S3.

Assays of leaf senescence and cell death.

Leaf senescence was assayed as described previously with minor modifications (5). The

photochemical efficiency of photosystem II (PSII) was deduced from chlorophyll fluorescence (6) using an Imaging-PAM chlorophyll fluorometer (Heinz Walz GmbH). The ratio of the maximum variable fluorescence to the maximum yield of fluorescence was used as a measure of photochemical efficiency of PSII (7). Chlorophyll was extracted from 3rd or 4th leaves by heating in 95% ethanol at 80 °C. Chlorophyll concentration per fresh weight of leaf tissue was calculated as previously described (8). For the detection of cell death, 3rd or 4th leaves of wild type and mutants at 14, 18, 22, and 26 days of leaf age were soaked in 0.05% trypan blue solution, incubated at 80 °C for 2 min, and then cleared with chloral hydrate (9). Representative leaf samples were mounted on glass slides and photographed using a Nikon SMZ-1500 stereomicroscope.

mRNA-sequencing and alignment of read sequences to *Arabidopsis* reference genome.

Total RNAs were prepared from leaves of *anac*017, *anac*082 and *anac*090 mutants and wild type (n = 3 for each). The RNA integrity number (RIN) of each sample was measured using the Agilent Technologies 2100 BioAnalyzer, and RINs for all the samples were larger than 7.8, which is suitable for mRNA-sequencing. According to the manufacturer's instructions, Poly(A) mRNA was isolated from the RNA (2 μg) and fragmented using Illumina Truseq™ Stranded mRNA LT Sample Prep Kit with poly-T oligo-attached magnetic beads. After the reverse transcription of the RNA fragments by using Superscript II reverse transcriptase (Life Technologies), the strand-specific cDNA libraries were constructed with adaptor-ligation and sequenced by Illumina HiSeq 2500 system. After the acquisition of read sequences for each sample, we checked the quality of raw sequences by FastQC (Babraham Bioinformatics) and trimmed the adapter sequences (TruSeq™ index adapter with the option "-a

AGATCGGAAGAGCACACGTCTGAACTCCAGTCAC", and the reverse complementary sequence of TruSeq™ universal adapter with the option "-a AGATCGGAAGAGCGTCGTGTAGGGAAAGAGTGTAGATCTCGGTGGTCGCCGTATCATT") using the cutadapter software. The remained reads were then aligned to the *Arabidopsis thaliana* genome (TAIR10) (10) using TopHat (11) with the default option. We then assembled the aligned reads into the annotated genes and calculated the fragments per kilobase per million mapped reads (FPKMs) using Cufflinks (12).

Identification of differentially expressed genes (DEGs).

On average, 34.9 million reads were acquired from each sample, and 99.0% of the reads were aligned to the *Arabidopsis* genome. The genes with FPKM >1 in at least one of the samples were determined to be expressed as previously described (13). After adding one to the FPKM values for the individual samples, we applied quantile normalization (14) to the $\log_2$-converted FPKM values. Using the normalized values, we performed the following comparisons to identify the DEGs using the integrative statistical test previously reported (15): 1) *anac017* vs. wild type, 2) *anac082* vs. wild type, and 3) *anac090* vs. wild type. For each gene, Student's *t*-test and $\log_2$-median-ratio test were conducted to obtain T-value and $\log_2$-median-ratio. Empirical null distributions for T-value and $\log_2$-median-ratios were generated by performing random sampling experiments 1,000 times and by applying Gaussian kernel density estimation to T-value and $\log_2$-median-ratios resulted from the random sampling experiments. For each gene, the adjusted *P* values for the observed T-value and $\log_2$-median-ratio were calculated using their corresponding empirical distributions by the two-tailed test. The *P* values were then combined to an overall *P* value by Stouffer's

method (16). The DEGs were identified as the genes with the overall *P* value <0.05 and absolute $\log_2$-median-ratio >0.475, which was the mean of 2.5th and 97.5th percentiles of the empirical distribution for the $\log_2$-median-ratio. To improve the specificity in the regulation of DEGs by ANAC017, ANAC082, and ANAC090, we removed the genes with no overall *P* values <0.01 in at least one of the comparisons and $\log_2$-median-ratios >0.475 in the comparisons with the overall *P* values >0.05. Moreover, to identify genes predominantly regulated by ANAC017, ANAC082, and ANAC090 among the DEGs from the three comparisons above, we also performed the comparisons shown in Fig. 4*A* using the same statistical method above. The enrichment analysis of gene ontology biological processes (GOBPs) was performed using the DAVID software (17). GOBPs enriched by the group were identified as the ones with *P* <0.05 computed from DAVID and the count ≥3.

GOBP-association analysis.

To select key processes represented by G1, we first built a network model describing the links among the 23 GOBPs enriched by G1. For a pair of the GOBPs (GOBP1 and GOBP2), when *n* and *m* DEGs were annotated with GOBP1 and GOBP2, respectively, with *k* shared DEGs annotated with both GOBP1 and GOBP2, we computed the similarity score as $2\times k/(n+m)$ (18) and connected the two GOBPs if the similarity score >0.3. To determine the cutoff, we estimated an empirical null distribution of the similarity score by performing random sampling experiments 1,000 times in each of which the same size of genes with G1 were randomly sampled from the genome and calculated the similarity scores for the 23 GOBPs using the randomly sampled genes. The cutoff of 0.3 was determined as the 95th percentile of the estimated null distribution. This procedure resulted in two connected subnetworks, called

Modules 1 and 2 (*SI Appendix*, Fig. S6*B* and *C*). In each module, the importance (weighted degree) of a GOBP was estimated by summing the similarity scores of its interactors. The GOBPs in each module was then ranked by their weighted degrees. On the other hand, the key GOBPs should be active during leaf aging. Thus, for a GOBP, we evaluated an activation degree in each module as the number of DEGs annotated with the GOBP that showed age-dependent up-regulation based on the previously reported time-course RNA-sequencing data during pre- and early-senescent stage (Mature-to-senescence stage; U1 and U2) (2). The GOBPs in each module was then ranked by the activation degrees. After summing the two ranks from the weighted and activation degrees, finally, the key GOBP in each module was selected as the top-ranked one based on the summed ranks.

Measurement of SA.

The 18-day-old 3rd or 4th leaves were extracted sequentially with 90 and 100% methanol (19). After centrifugation, supernatants were dried under liquid nitrogen. The residue was re-suspended either in 5% Trichloroacetic acid (TCA) or hot water at 80 °C to isolate free or total SA, respectively. Enzymatic hydrolysis was performed at 37 °C in 0.1 M sodium acetate buffer (pH 5) containing β-glucosidase (22 units mL^{-1}). The reaction was stopped with the addition of 10% TCA, and the resulting sample was centrifuged. The supernatant was partitioned with 2 volumes of a 1:1 (v/v) mixture of ethyl acetate and cyclopentane containing 1% (v/v) isopropanol. The resulting top organic phase was dried under liquid nitrogen and re-suspended by HPLC in the mobile phase of 40 mM sodium acetate (pH 3.5): methanol (75:25, v/v). As previously described (20), 20μl of the resulting sample were injected onto a Nova-Pak C18 60Å 4-mm Guard-Pak insert column (Waters) linked to a

Nova-Pak C18 60Å 4-mm column (3.9 x 300 mm; Waters) maintained at 40 °C. A linear segment gradient of methanol to 40 mm sodium acetate (pH 3.5) was applied at a constant flow rate of 1 mL/min as follows: 25% to 45% (w/v) methanol for 12 min, 45% to 100% (w/v) methanol for 6 min, and 100% to 25% (w/v) methanol in 5 min to re-equilibrate the column. A 474 scanning fluorescence detector (Waters) was used for SA quantitation with the gain set to 10, excitation wavelength at 295 nm, and emission wavelength at 405 nm.

Detection of superoxide and hydrogen peroxide.

The 3rd or 4th leaves of wild type, single and double mutants at 18 days of leaf age were floated in nitroblue tetrazolium (NBT) solution (0.5 mg/ml NBT, 10mM potassium phosphate pH 7.8, 10mM sodium azide) to detect superoxide. The leaves were vacuum-infiltrated with diaminobenzidine tetrahydrochloride (DAB) solution (0.5 mg/ml 3,3′-diaminobenzidine-4HCl, adjust pH 5.8) to detect hydrogen peroxide. After 6 hr incubation at room temperature under light, samples were cleared in destaining solution (ethanol:lactic acid:glycerol=3:1:1) at 60 °C overnight. Representative leaf samples were mounted on glass slides and photographed using a Nikon SMZ-1500 stereomicroscope.

Chromatin immunoprecipitation (ChIP)-qPCR.

Aerial parts of 2-week-old *pCsVMV:ANAC090-GFP* plants were harvested, fixed in 1% formaldehyde solution, and cross-linked under vacuum for 15 min. A final concentration of 0.25 M glycine was used to quench the formaldehyde under vacuum for 5 min. After washing twice with cold deionized water, the tissue was ground in liquid nitrogen, and extraction of

chromatin was performed as previously described (21). Prior to immunoprecipitation, 5 μg of anti-GFP monoclonal antibody (Abcam) was pre-incubated with 20 μl of protein A+G magnetic beads (Millipore) on a rotator at 4 °C overnight. Sonicated chromatin supernatant (250 μl) was diluted to 500 μl and pre-cleared with 20 μl of protein A+G magnetic beads at 4 °C for 1 hr. Supernatants were incubated with the prepared antibody-bound beads at 4 °C for 2 hr, and beads were washed sequentially with low-salt wash buffer, high-salt wash buffer, and TE buffer. Elution and reverse cross-linking were performed as previously described (21). The resulting immunoprecipitated DNA was purified with the Qiaquick PCR purification kit (Qiagen) and used for qPCR to examine the enrichment of target genes using the primers listed in *SI Appendix*, Table S3.

Transient expression assays.

Mesophyll protoplasts were isolated from mature leaves of wild type and transfected with constructs expressing HA- or GFP- tagged proteins as previously described (22). For *luciferase* (*LUC*) reporter constructs, the promoter of *PR1* was amplified from genomic DNA, cloned into *pCR-CCD_F* (23), and recombined into the gateway version of the *pGreen0800-LUC* vector (24), which contains *35Sp:RLuc* (Renilla *luciferase*) as an internal control. Transfected protoplasts with the *proPR1:LUC* reporter and an effector plasmid expressing ANAC090-HA or only HA were transferred to 96-well microplates containing 100 μM luciferin (Gold Biotechnology) or 10μM coelenterazine native (NanoLight Technology). Luminescence images were acquired after 16 hr incubation in dark and luminescence intensities were counted by MetaView system. For bimolecular fluorescence complementation (BiFC) analysis, cDNA fragments encoding *ANAC017*,

ANAC082, and *ANAC090* were obtained by PCR amplification and fused to plant expression vectors containing either N- or C-terminal fragments of the YFP fluorescent (YFP^N and YFP^C). Transfected protoplasts with different combinations of YFP^N- and YFP^C-tagged proteins (ANAC017, ANAC082, or ANAC090) along with the YFP^N control were incubated overnight at 22 °C under dim light (5 μE m^{-2} s^{-1}), and BiFC fluorescence was examined with a confocal laser scanning microscope (Carl Zeiss LSM 7 DUO).

Co-immunoprecipitation Assays.

Full-length cDNA fragments of ANAC017, ANAC082 and ANAC090 were inserted into a plant expression vector that contains two copies of HA-tag or GFP-tag driven by the *CsVMV* promoter. Mesophyll protoplasts were transfected with constructs expressing HA- and GFP-tagged proteins (ANAC017, ANAC082, or ANAC090) along with GFP control and incubated overnight at 22 °C under dim light (5 μE m^{-2} s^{-1}). Cells were harvested and lysed with IP buffer (50 mM Tris-HCl (pH 7.5), 150 mM NaCl, 10 mM EDTA, 0.1% Nonidet P-40, 50 μM MG132, 1 mM PMSF, and protease inhibitor cocktail). The supernatant was incubated with agarose-conjugated anti-GFP antibody (GFP-Trap, Chromotek) at 4 °C for 2 hr, and the pellet fraction was then washed four times with washing buffer (50 mM Tris-HCl (pH 7.5), 150 mM NaCl, 10 mM EDTA, 0.1 % Nonidet P-40, and protease inhibitor cocktail). The protein extracts and immunoprecipitated samples were heated at 95 °C for 5 min in SDS-PAGE sample loading buffer, separated on 10 % SDS-PAGE gels, and transferred to PVDF membranes. The blot was probed first with HRP-conjugated monoclonal anti-HA antibody (Roche), stripped with 0.2 N glycine (pH 3.0), and re-probed with HRP-conjugated monoclonal anti-GFP antibody (Santa Cruz Biotechnology).

Initially, we fused the GFP tag to the C-terminus of the three NAC proteins because the DNA-binding NAC domain is at their N-terminus. We observed proper localization of GFP fluorescence in plant cells. However, the ChIP assay was successful only for ANAC090-GFP, not for ANAC017-GFP and ANAC082-GFP. We then fused the GFP tag to the N-terminus of ANAC017 and ANAC082 and also observed proper localization of the GFP signal in plant cells. However, the ChIP assay also failed for GFP-ANAC017 and GFP-ANAC082. Close examination revealed that ANAC017-GFP and ANAC082-GFP proteins were degraded after protein extraction. This phenomenon might be due to the relatively long 'intrinsically disordered region (IDR)' in the proteins. The negative relationship between protein half-life and IDR length has been previously reported (van der Lee *et al*. 2014).

Supplementary Figures

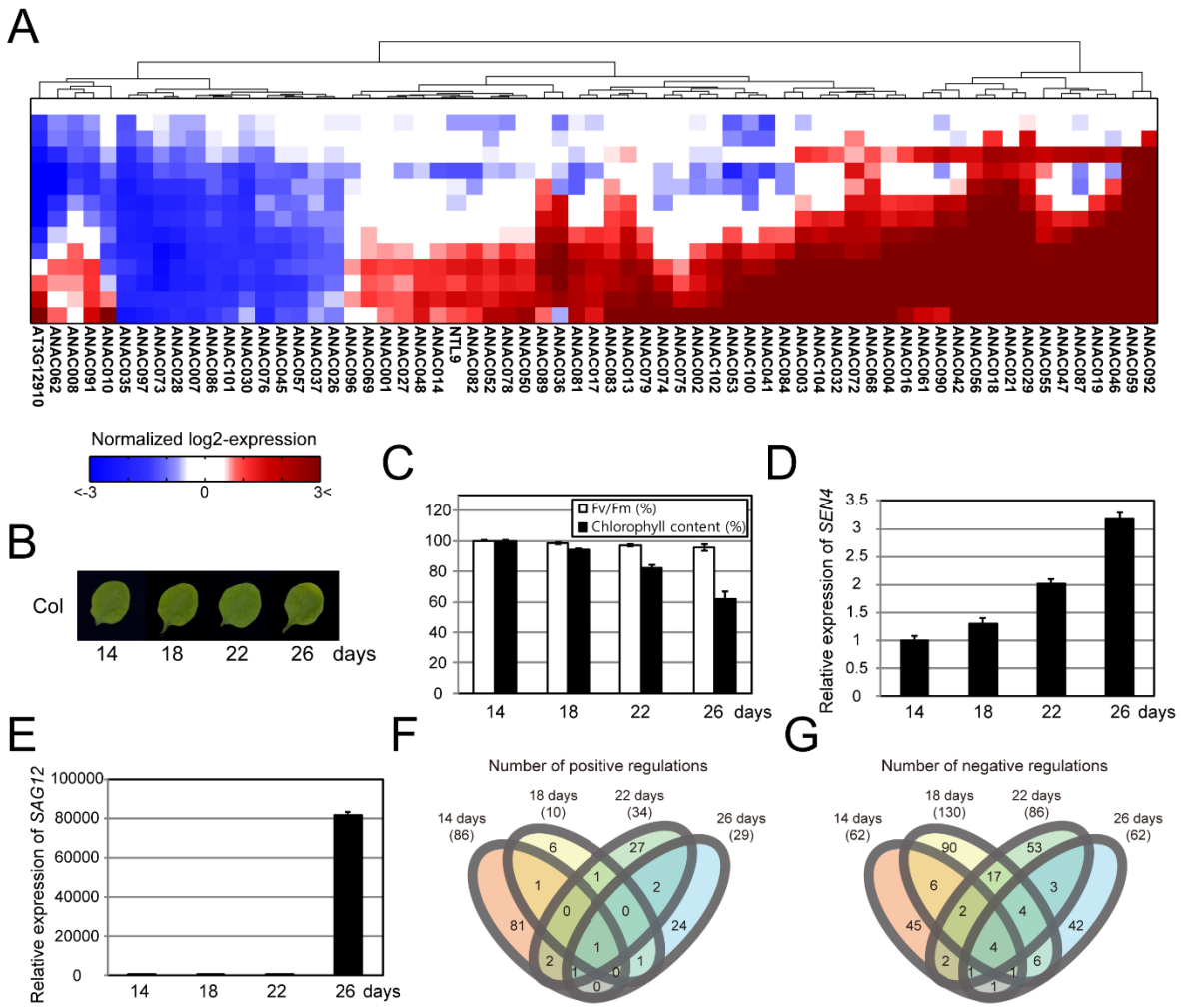

Fig. S1. Construction of time-evolving networks for aging-associated NACs. (*A*) 65 aging-associated *NACs*. The heat map shows temporal expression patterns of the 65 *NACs* in RNA-sequencing data reported by Woo *et al*. (2) (*Materials and Methods*). The dendrogram was obtained from hierarchical clustering of the temporal expression data using Euclidean distance as the dissimilarity measure and complete linkage. The colors represent up-regulation (red) and down-regulation (green) of NACs during leaf aging with respect to their

expression levels at 4 days of leaf age. The color bar denotes the gradient of log_2-fold-changes of NAC expression levels at individual time points with respect to those at 4 days of leaf age. (*B*) Leaf yellowing in wild type at four stages (14, 18, 22, and 26 days of leaf age). The third leaves at the indicated days after emergence (leaf age) were used. (*C*) Photochemical efficiency (Fv/Fm) of photosystem II and chlorophyll contents in wild-type leaves at four stages. Values are normalized by the values at 14 days of leaf age and then displayed as means ± SD (n > 12 leaves). (*D* and *E*) Relative mRNA expression levels of *SEN4* (*D*) and *SAG12* (*E*), representative senescence marker genes, with respect to those at 14 days of leaf age. The data were obtained from qRT-PCR analysis. Values are normalized to those of *ACT2* and then displayed as means ± SD (n = 2). (*F* and *G*) Relationships among positive (*F*) and negative (*G*) regulations at four stages. Numbers in parenthesis indicate the numbers of positive or negative regulations identified at each stage.

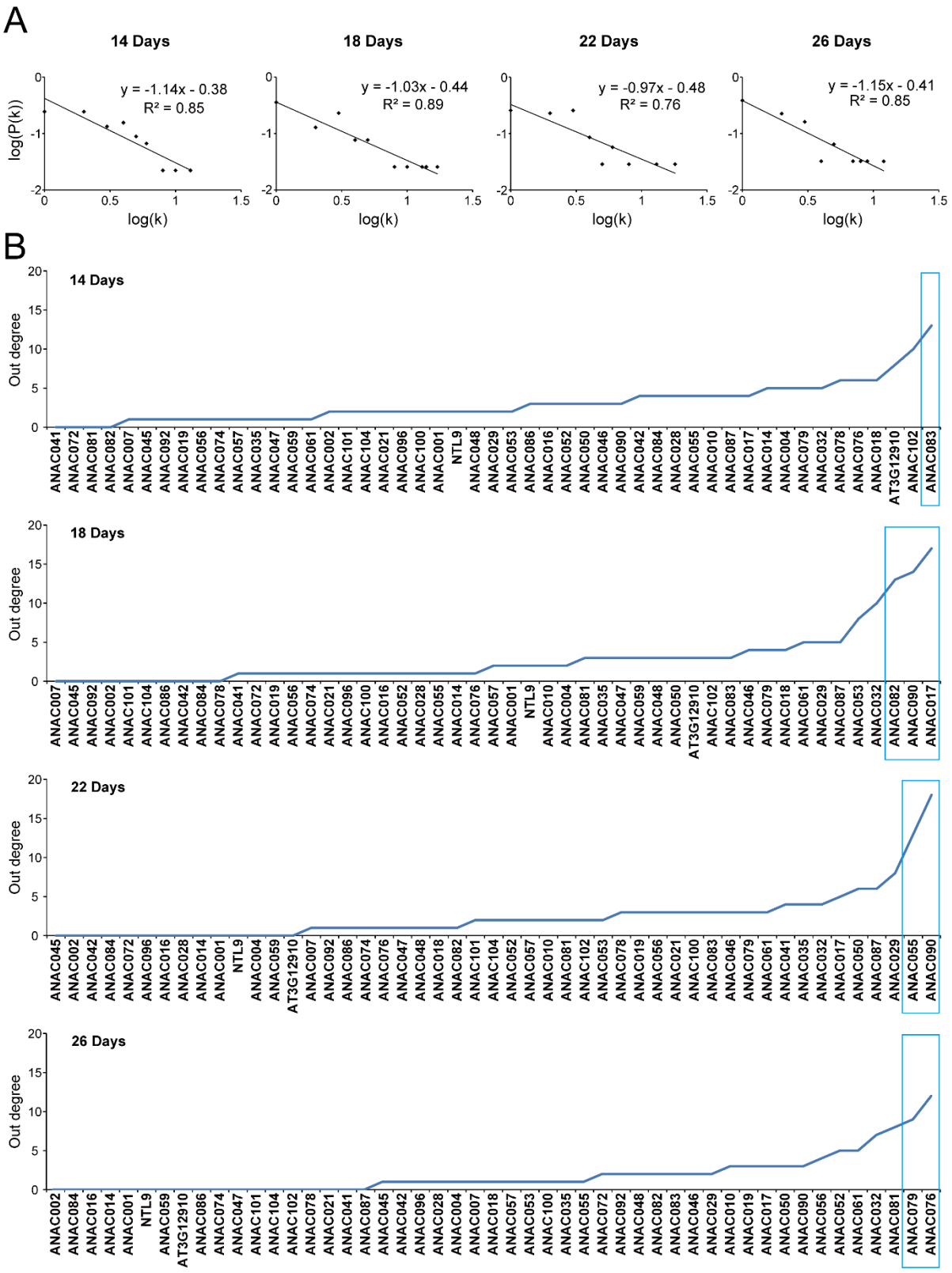
A
14 Days
y = -1.14x - 0.38
R² = 0.85
18 Days
y = -1.03x - 0.44
R² = 0.89
22 Days
y = -0.97x - 0.48
R² = 0.76
26 Days
y = -1.15x - 0.41
R² = 0.85
log(P(k))
log(k)
B
14 Days
Out degree
ANAC041 ANAC072 ANAC081 ANAC082 ANAC007 ANAC045 ANAC092 ANAC019 ANAC056 ANAC074 ANAC057 ANAC035 ANAC047 ANAC059 ANAC061 ANAC002 ANAC101 ANAC104 ANAC021 ANAC096 ANAC100 ANAC001 NTL9 ANAC048 ANAC029 ANAC053 ANAC086 ANAC016 ANAC052 ANAC050 ANAC046 ANAC090 ANAC042 ANAC084 ANAC028 ANAC055 ANAC010 ANAC087 ANAC017 ANAC014 ANAC004 ANAC079 ANAC032 ANAC078 ANAC076 ANAC018 AT3G12910 ANAC102 ANAC083
18 Days
Out degree
ANAC007 ANAC045 ANAC092 ANAC002 ANAC101 ANAC104 ANAC086 ANAC042 ANAC084 ANAC078 ANAC041 ANAC072 ANAC019 ANAC056 ANAC074 ANAC021 ANAC096 ANAC100 ANAC016 ANAC052 ANAC028 ANAC055 ANAC014 ANAC076 ANAC057 ANAC001 NTL9 ANAC010 ANAC004 ANAC081 ANAC035 ANAC047 ANAC059 ANAC048 ANAC050 AT3G12910 ANAC102 ANAC083 ANAC046 ANAC079 ANAC018 ANAC061 ANAC029 ANAC087 ANAC053 ANAC032 ANAC082 ANAC090 ANAC017
22 Days
Out degree
ANAC045 ANAC002 ANAC042 ANAC084 ANAC072 ANAC096 ANAC016 ANAC028 ANAC014 ANAC001 NTL9 ANAC004 ANAC059 AT3G12910 ANAC007 ANAC092 ANAC086 ANAC074 ANAC076 ANAC047 ANAC048 ANAC018 ANAC082 ANAC101 ANAC104 ANAC052 ANAC057 ANAC010 ANAC081 ANAC102 ANAC053 ANAC078 ANAC019 ANAC056 ANAC021 ANAC100 ANAC083 ANAC046 ANAC079 ANAC061 ANAC041 ANAC035 ANAC032 ANAC017 ANAC050 ANAC087 ANAC029 ANAC055 ANAC090
26 Days
Out degree
ANAC002 ANAC084 ANAC016 ANAC014 ANAC001 NTL9 ANAC059 AT3G12910 ANAC086 ANAC074 ANAC047 ANAC101 ANAC104 ANAC102 ANAC078 ANAC021 ANAC041 ANAC087 ANAC045 ANAC042 ANAC096 ANAC028 ANAC004 ANAC007 ANAC018 ANAC057 ANAC053 ANAC100 ANAC035 ANAC055 ANAC072 ANAC092 ANAC048 ANAC082 ANAC083 ANAC046 ANAC029 ANAC010 ANAC019 ANAC017 ANAC050 ANAC090 ANAC056 ANAC052 ANAC061 ANAC032 ANAC081 ANAC055 ANAC079 ANAC076

Fig. S2. Hub NACs in the time-evolving NAC networks. (*A*) Scale-free characteristics of genetic regulatory networks at four stages (14, 18, 22 and 26 days of leaf age). In each network, the scatter plot of log-probability-mass-function log($P(k)$) versus log-out-degrees log(k) shows that the out-degree distribution follows the power law, indicating scale-freeness of the network. The fitted equation and the goodness-of-fit (R^2) are shown for each network. (*B*) Identification of hub NACs in the genetic regulatory networks at four stages. NACs are sorted by their out-degrees in the network at the indicated stage. At each stage, we selected the hub NACs with significant ($P<1.0\times10^{-4}$; Methods) out-degrees, which were indicated by the box.

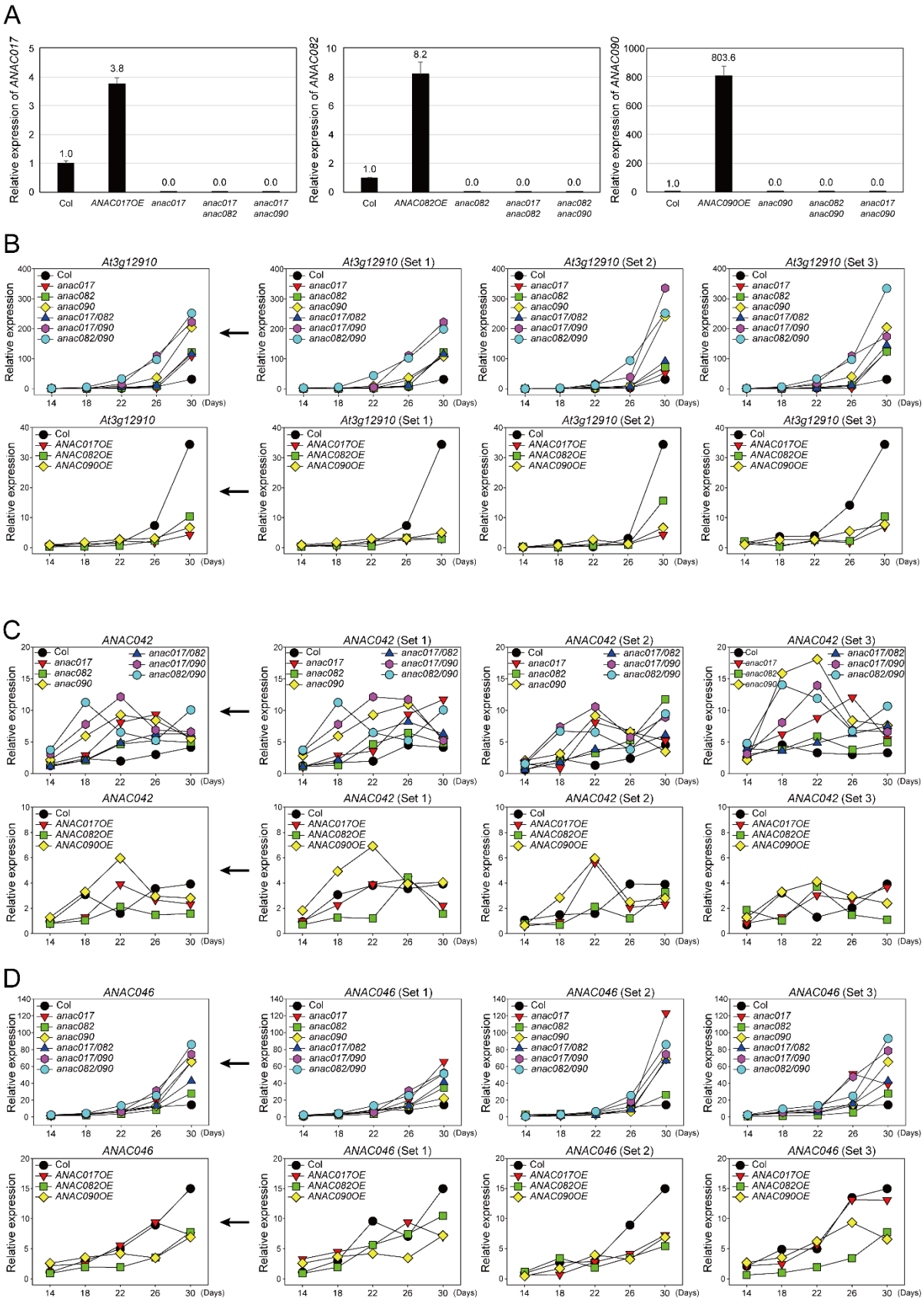
A
Relative expression of ANAC017
Col
ANAC017OE
anac017
anac017 anac082
anac017 anac090
Relative expression of ANAC082
ANAC082OE
anac082
anac017 anac082
anac082 anac090
Relative expression of ANAC090
ANAC090OE
anac090
anac082 anac090
anac017 anac090
B
At3g12910
At3g12910 (Set 1)
At3g12910 (Set 2)
At3g12910 (Set 3)
Relative expression
(Days)
Col
anac017
anac082
anac090
anac017/082
anac017/090
anac082/090
ANAC017OE
ANAC082OE
ANAC090OE
C
ANAC042
ANAC042 (Set 1)
ANAC042 (Set 2)
ANAC042 (Set 3)
D
ANAC046
ANAC046 (Set 1)
ANAC046 (Set 2)
ANAC046 (Set 3)

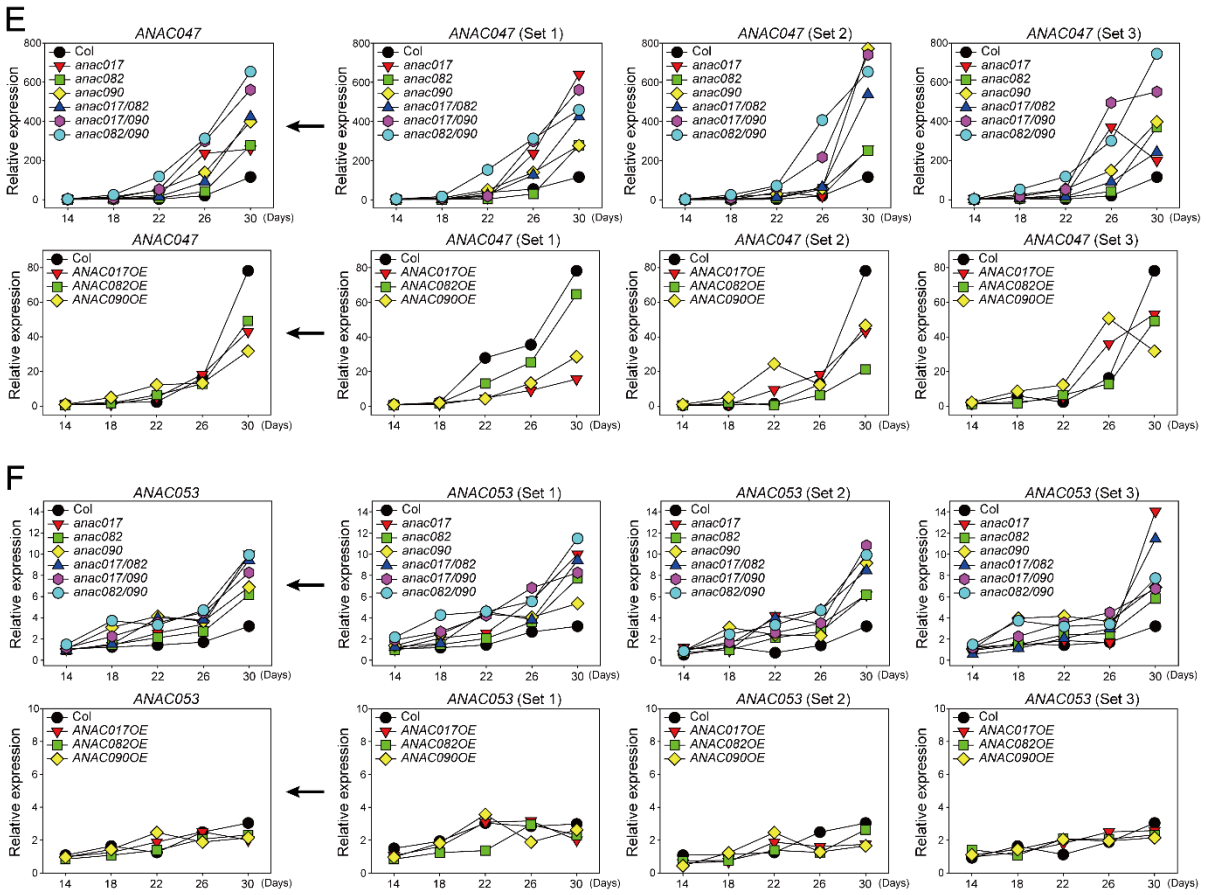
E
ANAC047
ANAC047 (Set 1)
ANAC047 (Set 2)
ANAC047 (Set 3)
Col
anac017
anac082
anac090
anac017/082
anac017/090
anac082/090
ANAC017OE
ANAC082OE
ANAC090OE
Relative expression
(Days)
F
ANAC053
ANAC053 (Set 1)
ANAC053 (Set 2)
ANAC053 (Set 3)

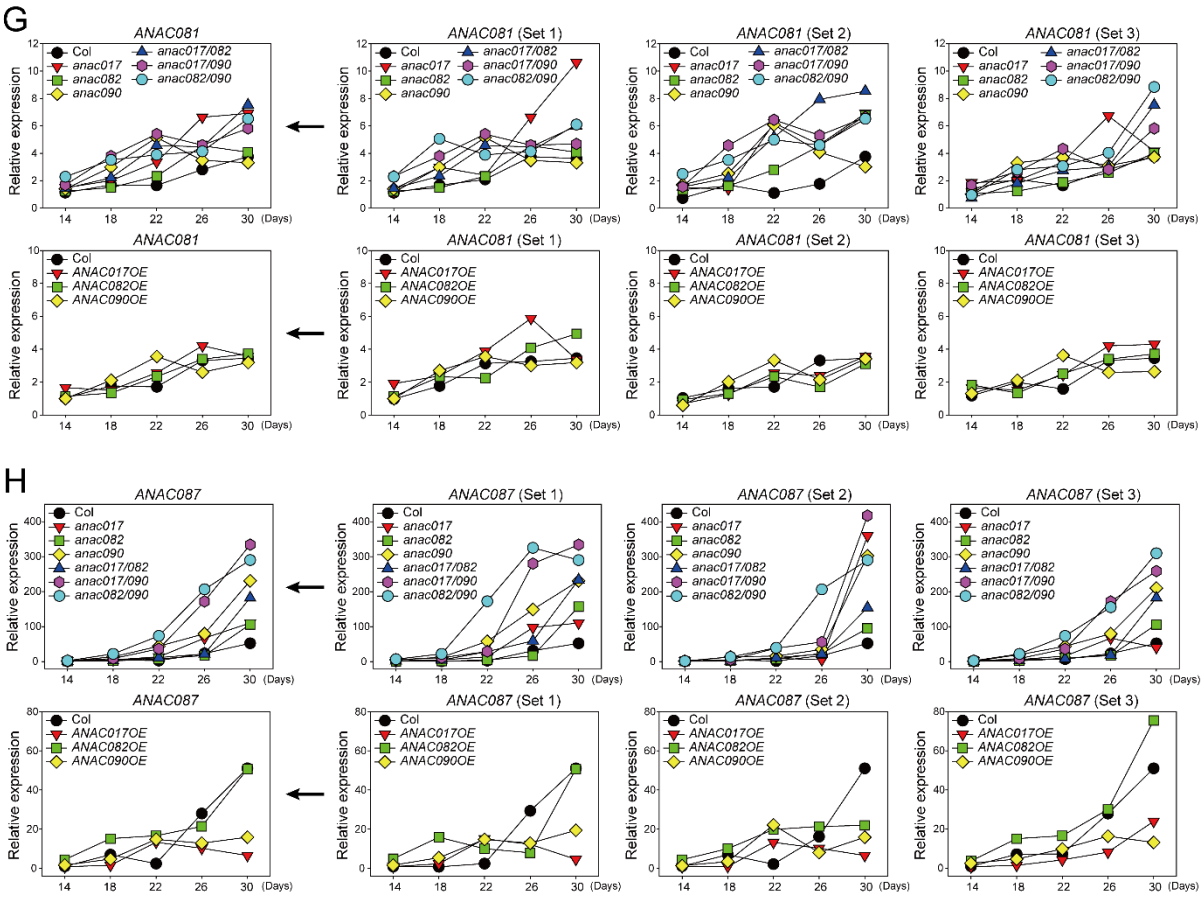
G
ANAC081
ANAC081 (Set 1)
ANAC081 (Set 2)
ANAC081 (Set 3)
Col
anac017
anac082
anac090
anac017/082
anac017/090
anac082/090
ANAC017OE
ANAC082OE
ANAC090OE
Relative expression
(Days)
H
ANAC087
ANAC087 (Set 1)
ANAC087 (Set 2)
ANAC087 (Set 3)

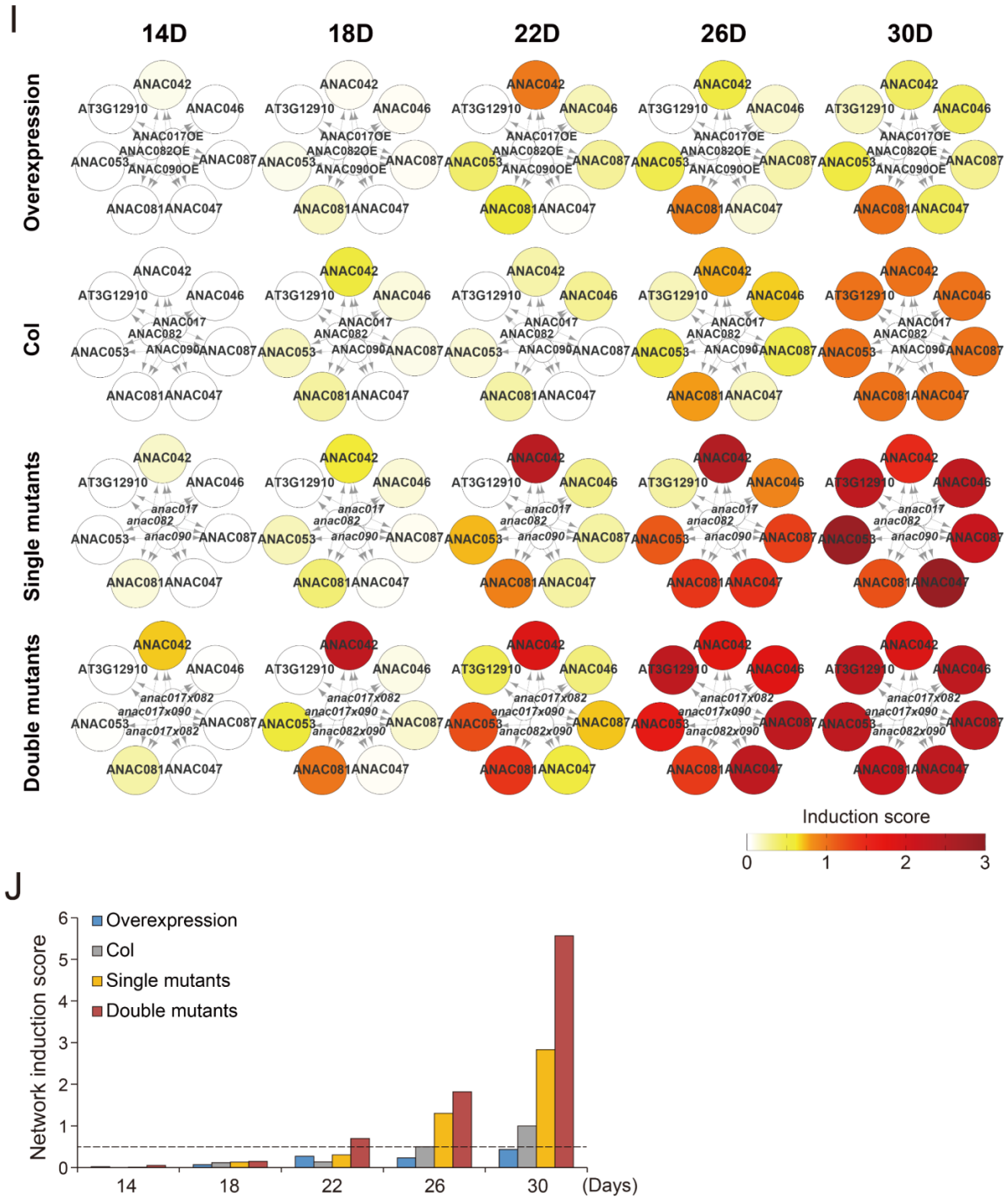

Fig. S3. Modulation of induction kinetics of target NACs by the NAC troika. (*A*) mRNA expression levels of *ANAC017*, *ANAC082*, and *ANAC090* in 26 day-old leaves from single

and double mutants, and overexpression plants of the NAC troika (*ANAC017*, *ANAC082*, and *ANAC090*). mRNA expression levels were measured by qRT-PCR. The mRNA expression levels of each gene were first normalized by those of *ACT2* and then further normalized with respect to the levels in wild type (Col). Values are means ± SD (n = 2). The mean relative expression levels were denoted above the bars. (*B-H*) Temporal mRNA expression patterns of seven target *NAC*s (*AT3G12910*, *ANAC042*, *ANAC046*, *ANAC047*, *ANAC053*, *ANAC081*, and *ANAC087*) that are regulated by more than two of the NAC troika in wild type, mutants, and overexpression plants. The median relative expression levels were calculated from the normalized expression levels of the three biological replicates as described in Methods. The median relative expression patterns in single or double mutants (*top*) and overexpression plants (*bottom*) are shown for *AT3G12910* (*B*), *ANAC042* (*C*), *ANAC046* (*D*), *ANAC047* (*E*), *ANAC053* (*F*), *ANAC081* (*G*) and *ANAC087* (*H*). The seven target *NAC*s showed faster induction in single and double mutants of the NAC troika, compared to that in wild type, but delayed induction in overexpression plants. (*I*) Time-evolving networks showing the induction scores of the seven target *NAC*s in wild type, mutants, and overexpression plants. The nodes in the boundary represent the seven target *NAC*s while the nodes in the center represent the deletion (*anac017*, *anac082*, and *anac090*) or overexpression (ANAC017OE, ANAC082OE, and ANAC090OE) of the NAC troika. For each node, we computed induction scores at individual stages in wild type, mutants, and overexpression plants as described in Methods. A darker red color indicates a higher induction score of the corresponding target NAC. The color bar indicates the gradient of the induction scores. The arrows indicate the effects of the deletion or overexpression of the NAC troika on the expression of the seven target genes. Consistent with the findings in (B)-(H), the induction of the nodes in the networks was faster in single and double mutants of the

NAC troika, compared to that in wild type, but delayed in overexpression plants. (*J*) Network-level induction scores representing the median expression levels of the seven target *NAC*s in wild type, single mutants, double mutants, and overexpression plants. The network-level induction score was estimated as the median induction score of target *NAC*s at each stage as described in Methods. Colors represent the network-level induction scores in the indicated mutant lines. The network induction was most significantly accelerated in double mutants, followed by single mutants, compared to wild type, but delayed in overexpression plants.

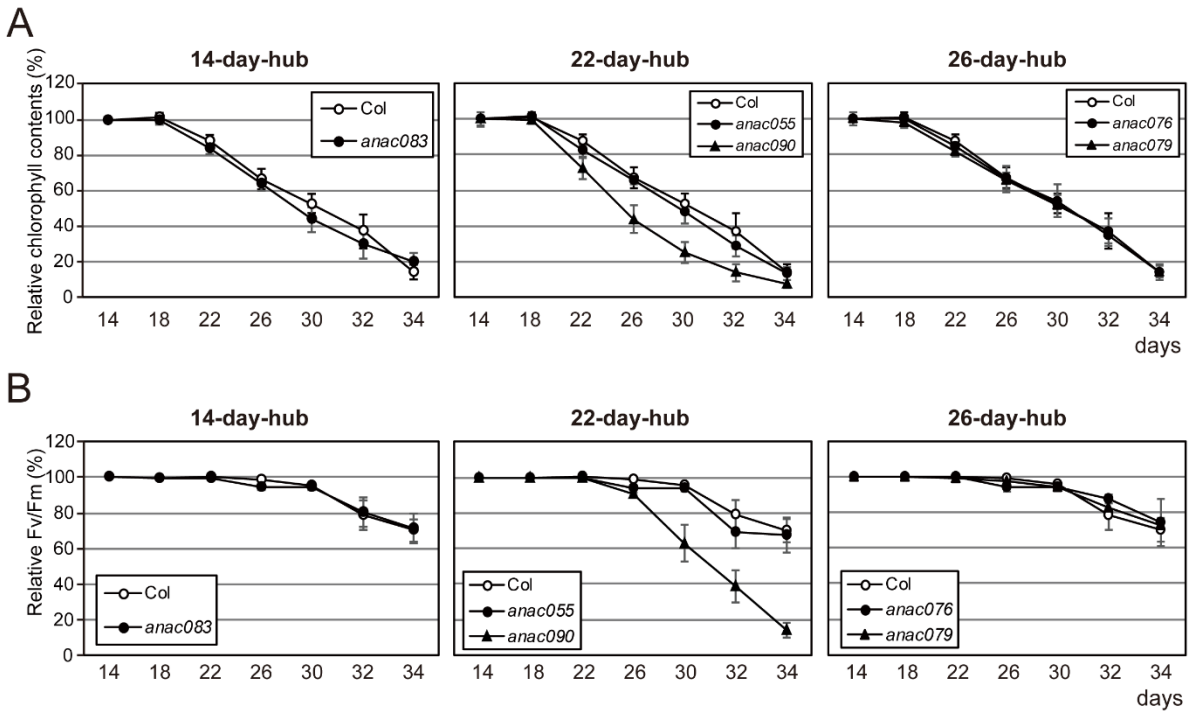

Fig. S4. Temporal changes of senescence phenotypes in mutants of hub NACs. Relative changes of chlorophyll contents (*top*) and photochemical efficiency (Fv/Fm; *bottom*) with respect to wild type (Col) were measured in mutants of the identified hub NACs at 14, 22, and 26 days of leaf age during leaf aging. Values are means ± SD ($n > 20$) and normalized to those at 14 days in individual mutants.

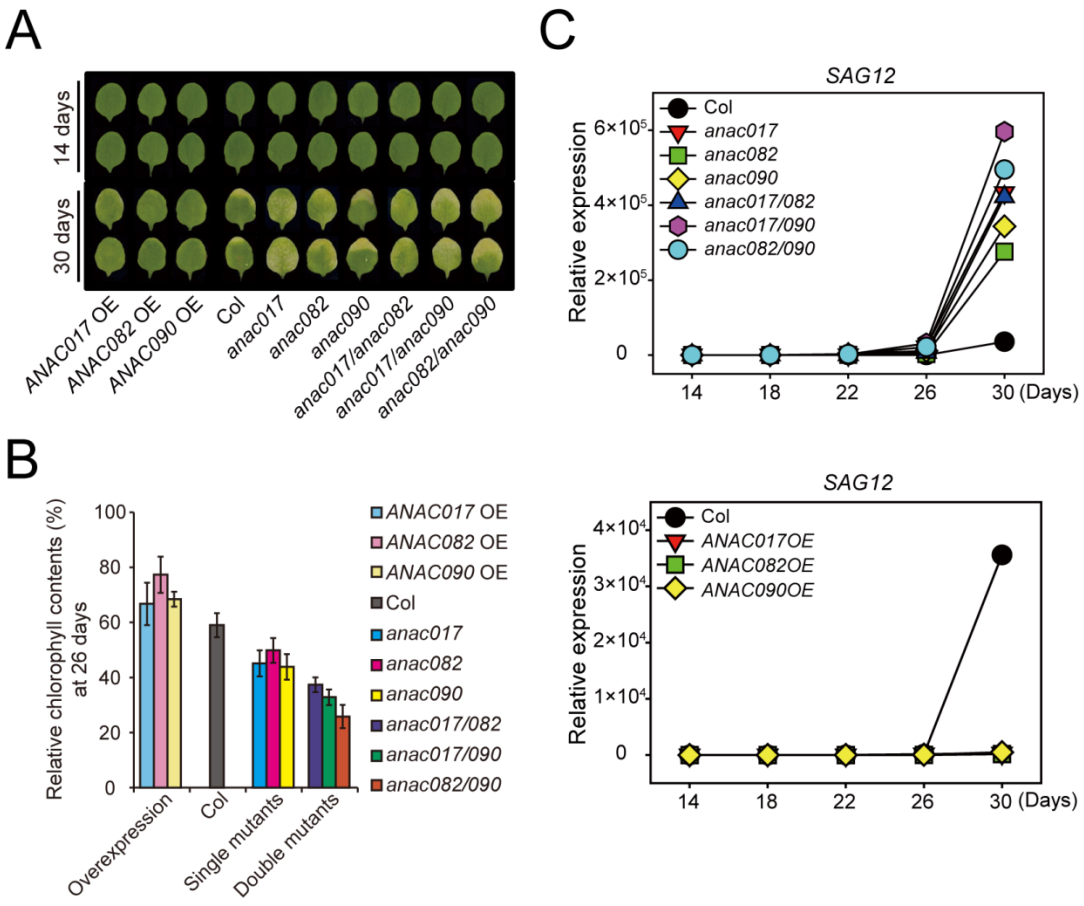

Fig. S5. Leaf senescence phenotypes of wild type, mutants, and overexpression plants of the NAC troika during leaf aging. (*A* and *B*) Leaf aging phenotypes measured at 14 days and 30 days (*A*) and relative chlorophyll contents measured at 26 days (*B*) in wild type, single mutants, double mutants, and overexpression plants. The relative chlorophyll contents in single mutants, double mutants, and overexpression plants with respect to 14 days are shown with standard deviation. Colors represent the data measured from the indicated mutants. (*C*) mRNA expression levels of *SAG12* in wild type, single mutants, double mutants, and overexpression plants at the indicated leaf age. The median expression levels obtained from the three biological replicates were displayed. Colors and symbols represent the data measured from the indicated mutants.

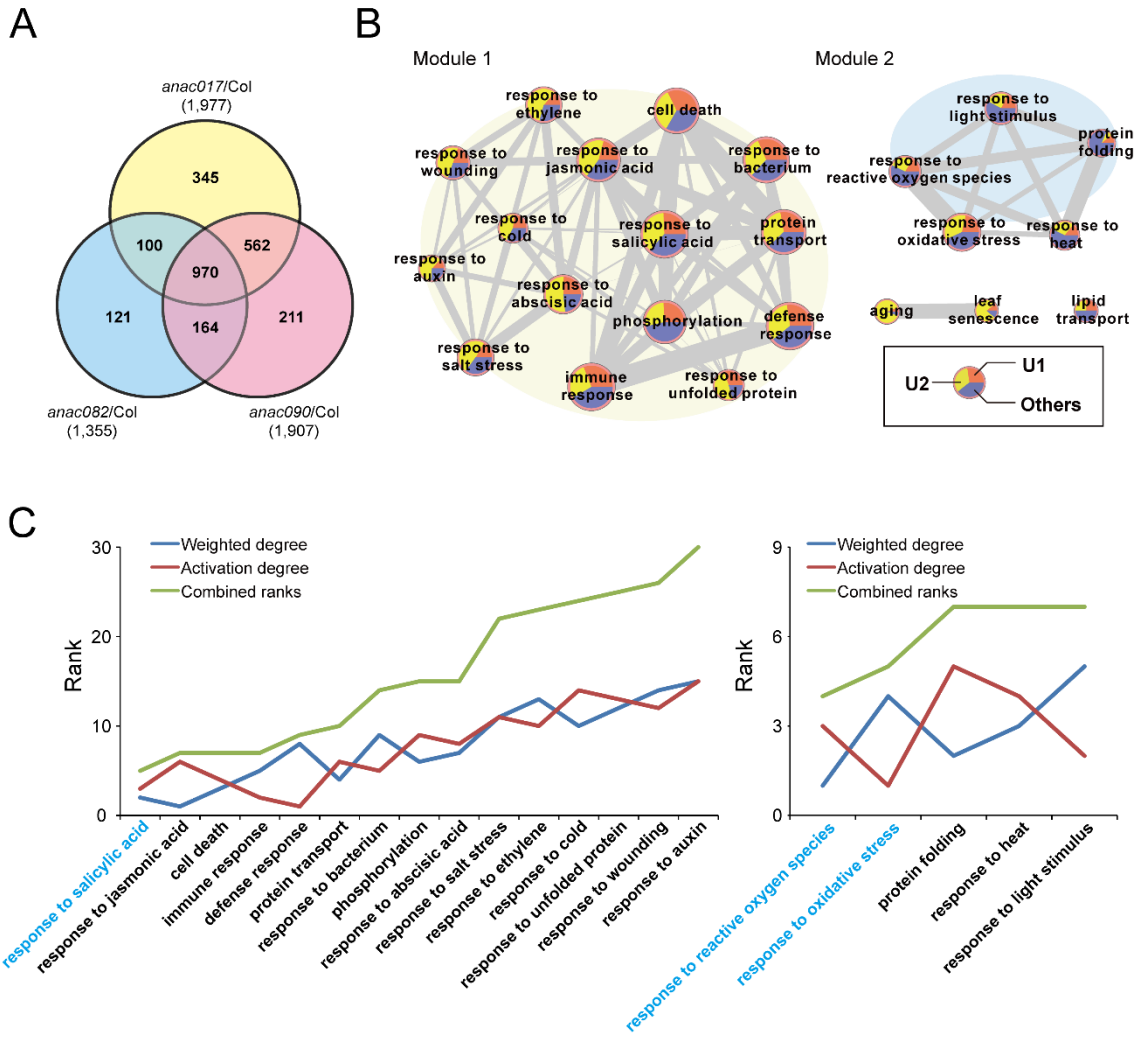

Fig. S6. Central senescence-promoting processes regulated by the NAC troika. (*A*) Relationships of genes affected by a NAC troika at 18 days. Numbers in parenthesis indicate DEGs in the following comparisons: 1) *anac017* vs. wild type (*anac017*/Col); 2) *anac082* vs. wild type (*anac082*/Col); and 3) *anac090* vs. wild type (*anac090*/Col). (*B*) GOBP association network showing relationships among pairs of the 23 GOBPs enriched by the genes in G1 (Fig. 3*B*). For each pair of the 23 GOBPs, we estimated a similarity score (edge weight) between the two GOBPs in the pair as an overlapping degree of G1 genes involved in the two GOBPs. Only the edges with the weights larger than a cutoff value of 0.3 (*Materials and*

Methods) are displayed, providing two modules (Modules 1 and 2). Edge thickness represents the similarity score between the corresponding two connected GOBPs. The node size describes the number of DEGs belonging to the corresponding GOBP. The pie chart of each node indicates proportion of the genes showing age-dependent up-regulation patterns (U1 and U2 for early and late up-regulation during the course of aging and Others for unchanged or other differential expression patterns than U1 and U2) previously reported by Woo *et al.*(*2*) during Mature-to-Senescence stage during leaf aging (see legend in the box). (*C*) Prioritization of the GOBPs in Modules 1 and 2 based on the two measures, the weighted degree (sum of similarity scores in each module) that indicates the importance of GOBP in each module and the activation degree (number of genes belonging to U1 and U2) that indicates the degree of aging-associated expression changes in each module. The GOBPs in Module 1 (*left*) and Module 2 (*right*) were then ranked by their weighted degrees (blue line) and also ranked by the activation degrees (red line). After combining the two ranks from the weighted and activation degrees, the GOBPs were sorted in an ascending manner based on the combined ranks (green line). Based on the combined ranks, responses to SA and oxidative/ROS stress were selected as the top-ranked GOBPs in Modules 1 and 2, respectively.

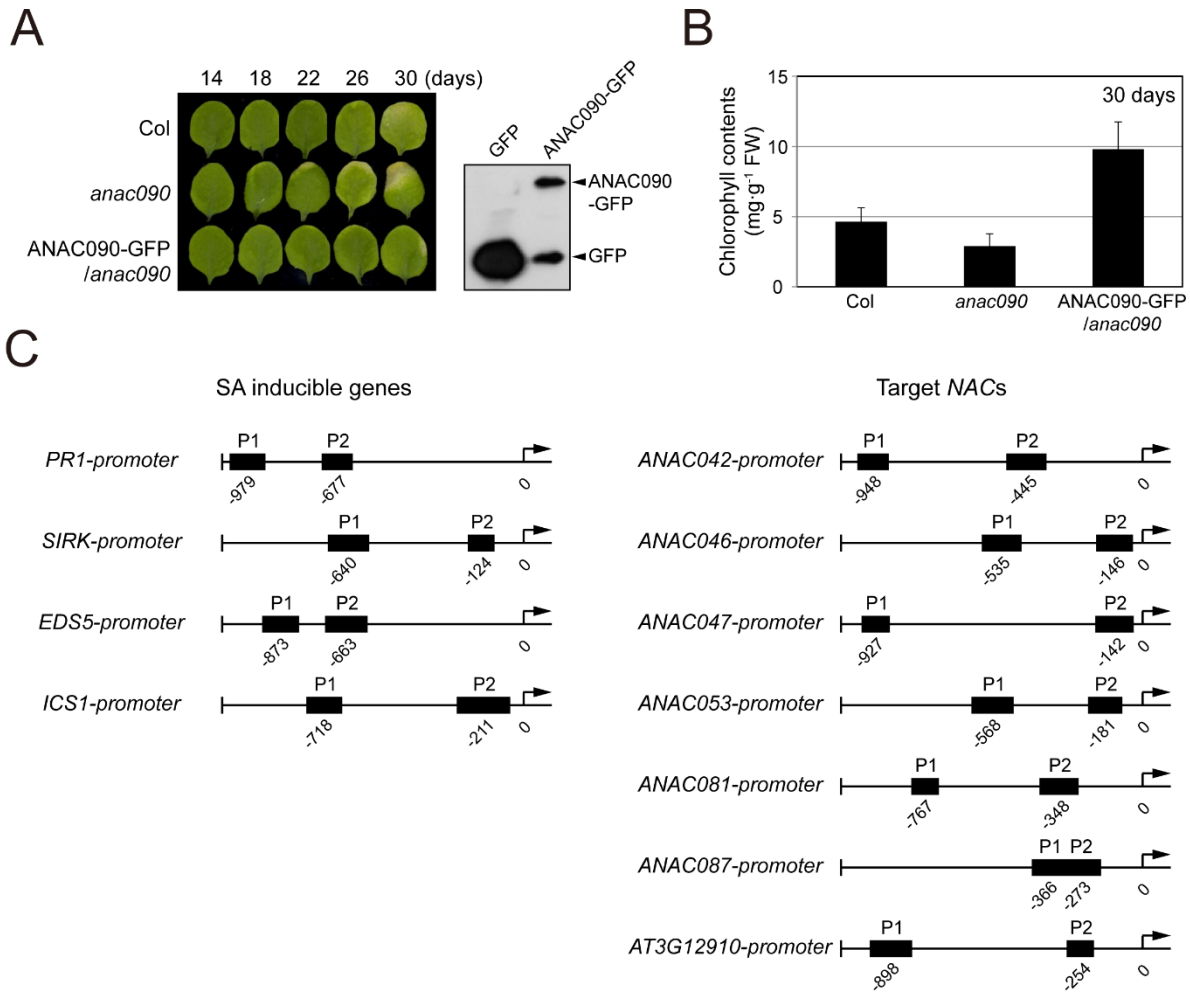

Fig. S7. *ANAC090-GFP* overexpression plants and NAC binding sites in promoter of target genes for ChIP-qPCR assay. (*A* and *B*) Leaf yellowing (*A*) and chlorophyll content (*B*) in wild type, *anac090*, and *ANAC090-GFP* overexpression plants at the indicated days of leaf age. (*C*) Locations of amplicons in the promoters of SA inducible genes (*PR1*, *EDS5*, *SIRK*, and *ICS1*) and downstream target *NACs* (*ANAC042*, *ANAC046*, *ANAC047*, ANAC053, *ANAC081*, *ANAC087*, and *At3g12910*) used for ChIP-qPCR experiments. For each gene, two amplicons (P1 and P2) were used, and they were determined as the regions containing putative NAC binding sites within the 1Kb upstream sequence after scanning NAC-binding sites using PlantPAN (version 2.0) (25).

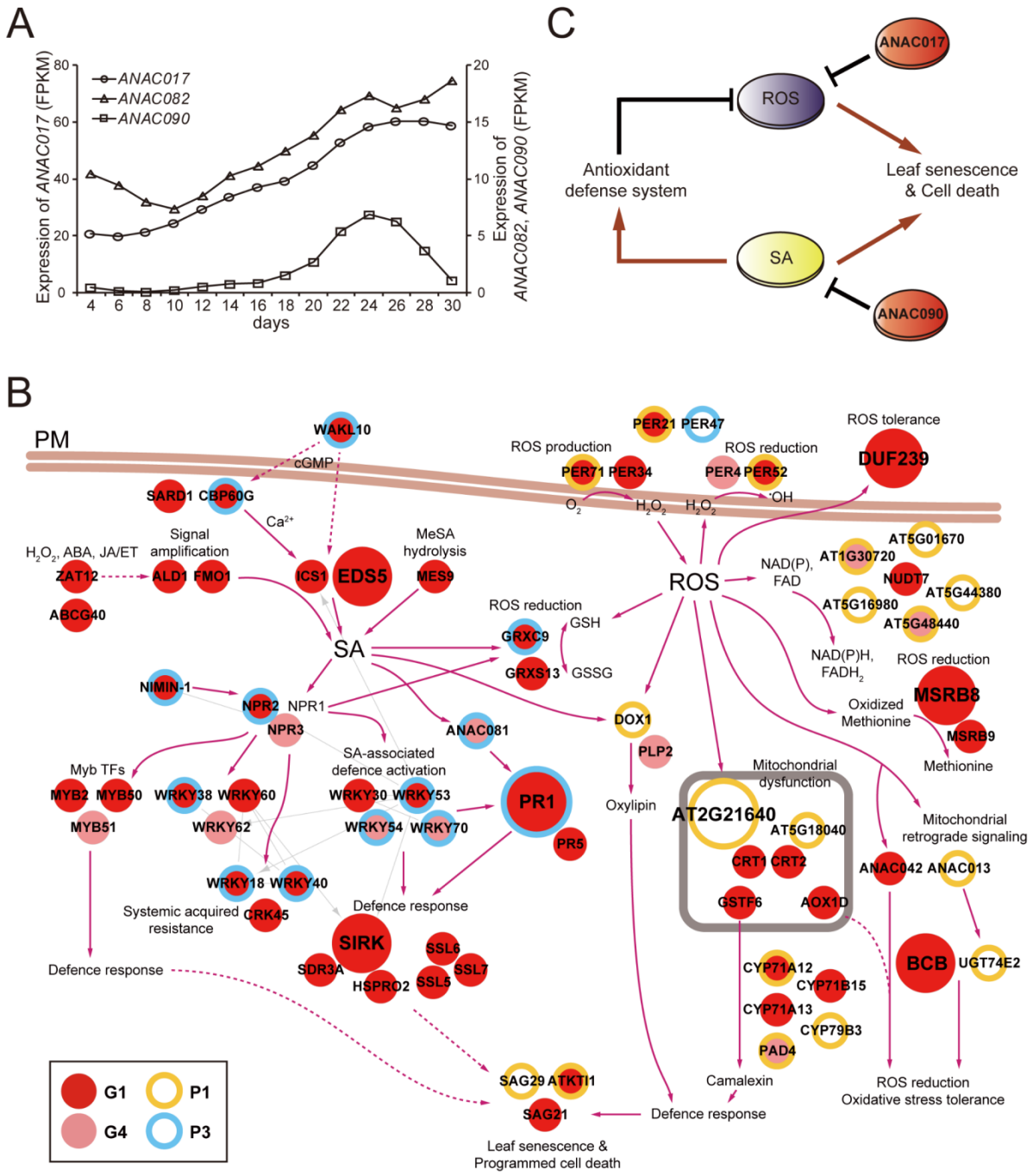
A
Expression of ANAC017 (FPKM)
Expression of ANAC082, ANAC090 (FPKM)
ANAC017
ANAC082
ANAC090
days
C
ANAC017
ROS
Antioxidant defense system
Leaf senescence & Cell death
SA
ANAC090
B
PM
WAKL10
cGMP
SARD1 CBP60G
Ca2+
Signal amplification
H2O2, ABA, JA/ET
ZAT12
ALD1 FMO1
ABCG40
ICS1
EDS5
MES9
MeSA hydrolysis
SA
NIMIN-1
NPR2 NPR1
NPR3
ANAC081
Myb TFs
MYB2 MYB50
MYB51
WRKY38 WRKY60
WRKY62
SA-associated defence activation
WRKY30 WRKY53
WRKY54 WRKY70
PR1
PR5
WRKY18 WRKY40
Systemic acquired resistance
CRK45
Defence response
SIRK
SDR3A
HSPRO2
SSL6
SSL5
SSL7
Defence response
PER21 PER47
ROS production
PER71 PER34
ROS reduction
PER4 PER52
ROS tolerance
DUF239
O2
H2O2
H2O2
OH
ROS
NAD(P), FAD
AT5G01670
AT1G30720
NUDT7
AT5G44380
AT5G16980
AT5G48440
NAD(P)H, FADH2
ROS reduction
GSH
GRXC9
GRXS13
GSSG
ROS reduction
MSRB8
Oxidized Methionine
MSRB9
Methionine
DOX1
PLP2
Oxylipin
Mitochondrial dysfunction
AT2G21640
AT5G18040
CRT1 CRT2
GSTF6
AOX1D
Mitochondrial retrograde signaling
ANAC042 ANAC013
BCB
UGT74E2
CYP71A12
CYP71B15
CYP71A13
CYP79B3
PAD4
Camalexin
ROS reduction
Oxidative stress tolerance
SAG29 ATKTI1
SAG21
Defence response
Leaf senescence & Programmed cell death
G1
P1
G4
P3
D
Relative Fv/Fm (%)
Col
cbnac/NTL9
anac081/ataf2
days

Fig. S8. Characteristics of the NAC troika. (*A*) Temporal mRNA expression patterns of the NAC troika during leaf aging. The left (y1) and right (y2) y-axes denote the expression levels of *ANAC017* (y1) and *ANAC082* and *ANAC090* (y2). (*B*) Network model describing interactions between SA and ROS response-related genes commonly and predominantly regulated by the NAC troika. Node colors represent genes with shared regulation by the NAC troika (G1 and G4 in red and pink, respectively), and node border colors represent genes with predominant regulation by ANAC017 (P1 in yellow) and ANAC090 (P3 in blue). Large nodes indicate the genes whose shared and predominant regulations were confirmed with qRT-PCR analyses in Fig. 3*C* and 4*E*, *F*. Gray lines with and without *arrows* denote protein-DNA and protein-protein interactions, respectively, which were obtained from interactome databases (Dataset S6). Solid and dotted red lines represent activations and functional associations, respectively, which were obtained from previous literatures (Dataset S6). Thick lines denote plasma (PM) and mitochondrial membranes. (*C*) A model for SA-ROS crosstalk that describes negative regulation of SA on ROS levels. (*D*) Relative changes of photochemical efficiency (Fv/Fm) in *cbnac/ntl9* and *anac081/ataf2* mutants during leaf aging. Values are means ± SD ($n > 20$) and normalized to those at 14 days in individual mutants.

Supplementary Tables

Table S1. Knockout mutants of 49 aging-associated NACs. For each knockout mutant, NAC name, TAIR accession ID, and Mutant ID reported at the *Arabidopsis* biological resource center are shown together with left primer (5'-3') and right primer (5'-3') sequences. The mutants were generated using T-DNA insertion except for *ore1-2* (*ANAC092*) that was generated by deletion by fast neutron.

Genes	TAIR accession ID	Mutant ID	Left primer (5'-3')	Right primer (5'-3')
ANAC001	AT1G01010	SALK_128571	AACCATACCAATTAAACCGGAG	CGCATCATCACCCTTGTACTC
ANAC002	AT1G01720	SALK_057618	TCCCAGGGACAGAAAATATCC	AAATATTAAATTGATTGCGGCAC
ANAC004	AT1G02230	SALK_054446	CCCTCTTGTGAACAGTTCTGG	TCCAACTTTCTCTTCTCGGAC
ANAC007	AT1G12260	SALK_145159	TGGTACTCAGCATTGCTTGTG	TACAAGATTGAGCCATGGGAC
ANAC010	AT1G28470	SALK_000287	TGGTTATCGCGATTTCATTTC	CTCGAGGTTAAAGTTACGCCC
ANAC014	AT1G33060	SALK_024241	AGCATCTAGTGGTGGTGGTTG	TCAGACCAACGGATGAAGAAC
ANAC016	AT1G34180	SALK_001597	CTGATGAGAACTGGCTCCTTG	TCTCAATGAAATCCCAGATGC
ANAC017	AT1G34190	SALK_022174	TGTTACGTAGATGGCGGATTC	TTCTCAGTTGAAGAAGCTCCG
ANAC018	AT1G52880	SALK_201909	TTTTCTTGTTGCCGAAGTCAC	CCTACACATATGGGTCAAAACG
ANAC019	AT1G52890	SALK_096295	TCAATGAACTCAAGGGATTGC	ATGCGGTTTGGGTTAGAAAAC
ANAC021	AT1G56010	SALK_052190	GAAGGACGATGAGCTTGTCTG	CATGTGATTAAATGTTAGCGCC
ANAC028	AT1G65910	SALK_146108	AATGCGAACCTTGGGATTTAC	AAGACGGTACTCGTGCATGAC
ANAC029	AT1G69490	SALK_005010	CTTTTTAACCGTGGCTGTTTG	GTCCCCGAACCAACTAGACTC
ANAC032	AT1G77450	SALK_012253	ACCAACAATTGTGGAAGCAAG	CTCTCCATTTGGAGGTTTTCC
ANAC035	AT2G02450	GABI_817A02	TTTAACGTGCATGAGATGGTG	AAGAAACTAAAGAGGGAGAAGCG
ANAC041	AT2G33480	SALK_066378	TGTGATTCAAGGGTGGAAGTC	TTGTTCCGTTTGGTGGTTTAC
ANAC042	AT2G43000	SALK_205572	CAAAAAGTTGGGTCCATTTTG	TGAAGAAGAAAACGAAGCACC
ANAC045	AT3G03200	SALK_111675	TTACCTCCAGGTTTCCGATTC	CACACGACAAAGTGCATATGC
ANAC046	AT3G04060	SK2690	TTCGGTTTCACCCTACTGATG	CCGGTTTCTTGAGACACACTC
ANAC047	AT3G04070	GABI_343D11	TGAGTTCCTGGTTCAGGAAAC	CATCAGCTAAGGCTCCATTTG
ANAC048	AT3G04420	GABI_687F10	GGGAGAAACTACCGTCACATG	AAAACGAGCAATCAAATCACG
ANAC050	AT3G10480	SALK_026244	TCCTAGCGTTTGTAAATCTTTGAAC	TTCATTTCCTGATCCACAAGC
ANAC052	AT3G10490	SAIL_783_C03	AGCCTGGATTCCATCTCTCTC	TTTCCTGAACCACAAGCAAAC

ANAC053	AT3G10500	SALK_009578	TCTTCATTTCCCATCAGTTGC	TGGTGGGAAATAGACAAGTCG
ANAC055	AT3G15500	SALK_014331	TAAACGATGAGCGATAGCGAG	AAAGGAACCAAAACCAATTGG
ANAC056	AT3G15510	SALK_046955	GTCAGCGTTATTGTCGTGATCTAC	GACGAAGAGCTTGTTGTTCACTAC
ANAC057	AT3G17730	SALK_206572	CTAGGCGATTTGCTTCATCTG	ATAACCCAATCCGTACGGATC
ANAC059	AT3G29035	GABI_778C04	TGGTTTAAGAACGAATCGTGC	CAATGGATTTCAAATGGCAAG
ANAC061	AT3G44350	SALK_038220	AGGTTGATATTGTGGCACGAG	AGAGGAGGCAGACCAAGTAGG
ANAC072	AT4G27410	SALK_063576	AGTGATCGAGTGCTTCAGGAC	ACTCGTGCATAATCCAGTTGG
ANAC074	AT4G28530	GABI_224H04	CATGCATGATTCCTCACAATG	GAGAGCAATAATTTCCTCCGC
ANAC076	AT4G36160	SALK_022124	CGAGACAAGGCTGTTTACGAC	CCTTTAGGCCAATGTCAAACA
ANAC078	AT5G04410	SAIL_573_G02	AAAGAGGCAGTGGAGGAAAAG	AGAGTGGGGGAAACATGTTCT
ANAC079	AT5G07680	SALK_040204	AACCCACCACAATGCATTAAC	AGAGATCTTCCGAGGCAAATC
ANAC081	AT5G08790	SALK_136355	CCAGATCCAGCTGAAATTGAA	AATCATCCTCTTGCAATGTCG
ANAC082	AT5G09330	GABI_282H08	GAGCAGTGTGGTCTTGTAGCC	GTGTGTTACTGTCCTGCCTGC
ANAC083	AT5G13180	GABI_799H09	AATAATCTCACCGTCACGTGC	TGATAAACGGGTTGTGACCTC
ANAC084	AT5G14000	SAIL_900_G07	GGCAGTGTTGTGTCTCCTCTC	GTCCCCTGAAAGCAAAACTTC
ANAC086	AT5G17260	SALK_142816	AAGTACCCCAATGGTTCAAGG	GCGAGTTTTCTACTCGCAATG
ANAC087	AT5G18270	GABI_622H06	TCGTTGGGATGAAGAAAACAC	TCCCAAATTATCACAATCCTTTC
ANAC090	AT5G22380	SALK_206203	CCACATCGGTTCTGATAGTCC	GAATTGGTTCGGGTTTGGTAT
ANAC092	AT5G39610	*ore1-2*	-	-
ANAC096	AT5G46590	SALK_078797	TGCATGAATATCGACTATGCG	ACCGAATAAACCGGTTTGATC
ANAC100	AT5G61430	SALK_203888	CCATGAGGATGAAAACAATGG	AGACAGAAAGTATCCCACCGG
ANAC101	AT5G62380	GABI_567F08	ACACGAACCAATAGAGCAACG	AAGCATTCATCGAAACCATTG
ANAC102	AT5G63790	SALK_030702	CTTGAGCATCTTGAGTCCGAC	TCTATCTTTGCCGGAGATGTG
ANAC104	AT5G64530	SALK_057218	GAAGTACCATTGCCTCCCTTC	GATGAAGAGCTCGTCGTTCAC
AT3G12910	AT3G12910	SALK_016619	TAAGACCGAACCGAGTGACTG	CACCTAATGGGCTTTGTTTCC
NTL9	AT4G35580	SALK_055735	TGCATAATCCAATTAGTCCGC	TGGCCCTCAAAAAGTTACATG

Table S2. Groups of DEGs categorized by their differential expression patterns in the comparisons of mutants versus wild type. Colors represent up- (red) or down-regulation (green) of DEGs in the three comparisons: 1) *anac017* vs. wild type (*anac017*/Col); 2) *anac082* vs. wild type (*anac082*/Col); and 3) *anac090* vs. wild type (*anac090*/Col). Blanks denote no significant changes in the corresponding comparisons. The groups were sorted by the number of genes (Count) in the groups.

Group	*anac017*/Col	*anac082*/Col	*anac090*/Col	Count
G1	Up	Up	Up	638
G2	Down		Down	328
G3	Down	Down	Down	328
G4	Up		Up	225
G5	Up			200
G6	Down			145
G7			Down	107
G8			Up	104
G9		Up	Up	95
G10		Up		67
G11		Down	Down	67
G12	Up	Up		60
G13		Down		54
G14	Down	Down		36
G15	Up		Down	8
G16	Up	Down		3
G17	Up	Up	Down	2
G18		Up	Down	2
G19	Down	Up	Down	2
G20	Down	Up		1
G21	Down		Up	1

Table S3. Primers used in this study.

Name	Forward primers (5'-3')	Reverse primers (5'-3')	Purpose
ANAC017	TGGTGCTCCGTTTCAAGAAGA	CCTCTCATCCACACGACGAG	qRT-PCR
ANAC082	CAAGACCTCACTGCTCCATTTA	GTCATTGCGATTCCCAGTTTG	qRT-PCR
ANAC090	CATCGTGTCATTCCCGTACTT	GCAATGGTTCTTCTTCGTGC	qRT-PCR
SEN4	CGTCGATGACACACCCATTAGAG	CATCGGCTTGTTCTTTGGAAAC	qRT-PCR
SAG12	AAAGGAGCTGTGACCCCTATCAA	CCAACAACATCCGCAGCTG	qRT-PCR
At2g21640	GGCTTCCCAGACAAATCAAACC	CGTTATCATCCTTCACCCTCTTC	qRT-PCR
PR1	GTTGCAGCCTATGCTCGGAG	CCGCTACCCCAGGCTAAGTT	qRT-PCR
EDS5	TGCATTGCCCATGACAGTAT	ATTGAAATCCGACGAGAACG	qRT-PCR
SIRK	GGCTTTAGCTTTGTTCCGGC	TTCAACGGCCCATTCCTCTC	qRT-PCR
ICS1	GCTTGGCTAGCACAGTTACAGC	CACTGCAGACACCTAATTGAGTCC	qRT-PCR
DUF239	GATGTAGCAACTCCCAGCGA	ACCTGCCAACCAGCTTCAAT	qRT-PCR
BCB	GTGGGACCACAACACCTTCA	ATGAGGAAGCGGCATTTCCA	qRT-PCR
MSRB8	GCGGCTGCAGTTCCATCAAG	CAGAACAGCACGCCACTCTT	qRT-PCR
ANAC004	TCGCAGCGATTACACACCTC	GCTGGACTGTTGAGTCAGGA	qRT-PCR
ANAC016	ATTCACTTCACAGTCAACAGGTG	GCTGATGAGAACTGGCTCCT	qRT-PCR
AT3G12910	CGAGTGACTGGTTCCGGTTT	ACCGGGGATTGTGTCATTGG	qRT-PCR
ANAC042	ACCAAAACCGATTGGATGAT	TTCTGCAAAGTGTCCATACCTC	qRT-PCR
ANAC046	TCCGGGTTTCTTGGGTCAAC	ATGGACCGAGTGGTAAGGGA	qRT-PCR
ANAC047	TCATCCAACAGATGAAGAACTCA	CTCCCCAAATGGAGCCTTAG	qRT-PCR
ANAC053	GCAACAGAGTTTGAGCCAGA	GCAGGAATAGCACCCAACAT	qRT-PCR
ANAC081	ACCACGACAATGGCTGAACA	CACCTGAGCTGCTGGAATCA	qRT-PCR
ANAC087	AGTGTGAGCCTTGGGATTTG	CCCAGTCGGATACTTCCTGT	qRT-PCR
ACTIN 2	TCCCTCAGCACATTCCAGCAGAT	AACGATTCCTGGACCTGCCTCATC	qRT-PCR
ANAC017	GAGAGTCGACATGGCGGATTCTTCACCC	GAGAAGGCCTGTCTTTCAAGAGAAGACTTCTACCTG	Cloning
ANAC082	GAGAGTCGACATGGGGAAAACTCAACTCGC	GAGAAGGCCTCATTTTTGGTCTATGTCTCA	Cloning
ANAC090	ACTAGTATGGCCGATGAGGTCACAATC	AGGCCTAGGCCAAGTCAGCTGTTCC	Cloning
ANAC017-BiFC	AGATCTATGGCGGATTCTTCACCCGATTC	GAGAAGGCCTGTCTTTCAAGAGAAGACTTCTACCTG	Cloning
ANAC082-BiFC	GGATCCATGGGGAAAACTCAACTCGCTCCT	AGGCCTCATTTTTGGTCTATGTCTCATGG	Cloning
ANAC090-BiFC	GGATCCATGGCCGATGAGGTCACAATC	AGGCCT AGGCCAAGTCAGCTGTTCC	Cloning
ProPR1	CCCGGGTTCGGAGGGAGTATATGTTATTG	CTCGAGGATTTTGGGGTTCGTAAACATCG	Cloning
PR1-P1	CTGATTCGGAGGGAGTATATGTTATT	TTGTACCGCCTTCGTATATCATT	ChIP-qPCR
PR1-P2	TGACTGTTTCTCTACGTCACTATTT	TGCATATGAGTATCTCTATCACTCTTG	ChIP-qPCR

SIRK1-P1	CATCGTTGAAACTTGAAAGTGATGA	GTTGAATATCAATGTGTTACGGTGA	ChIP-qPCR
SIRK1-P2	AAGCGTTGACATATATTACGTCCT	TGTTGATAGTCAACCAACCATCT	ChIP-qPCR
EDS5-P1	AATGGAACATAACTTACGACGA	TTTGCTTTCGCAGTGTAGTTAC	ChIP-qPCR
EDS5-P2	CTTGCGTTATGGTTGGGTTTTC	AAATTAGGAAACAAGTCTCTCTCG	ChIP-qPCR
ICS1-P1	AAGGAGCATGCGTGTAATGCCA	CGTTTGATACGGAAGCGGTTTGCAC	ChIP-qPCR
ICS1-P2	TGCACGACTAACTTTAGAAAAATGT	AGGGGACTGATGTAGCAGGGGC	ChIP-qPCR
ANAC042-P1	TGGAATGCAGTTGAAGGAATTG	GCCCTCCTTTGTGGACTAAT	ChIP-qPCR
ANAC042-P2	AACTTTCAAACACAGCCAAAAC	CTAGAGAATCTGAAACCTCCAA	ChIP-qPCR
ANAC046-P1	TTCTGGTGGTTGGCTAAGGAAC	TTTAGATCCATAGGGTGACACG	ChIP-qPCR
ANAC046-P2	CAAGTAAGGAAGTTGCTTAGAGC	CTTTATATAGAGGAAGATAAGAGC	ChIP-qPCR
ANAC047-P1	GGGCTTACGTGGATATGGTTAG	GTTAGAGAAGTGGACCCAAATGA	ChIP-qPCR
ANAC047-P2	TCCTCCGGTCTACTTTACAGA	TTTGAGGGCAATTTATGGTGTG	ChIP-qPCR
ANAC053-P1	CATAACACACTGAGCCTTCTCT	ACCGGAGACCGAACATAATTC	ChIP-qPCR
ANAC053-P2	CGAACCAACCAACTACCTCAA	GTGACTGGCTGTGACTGTTT	ChIP-qPCR
ANAC081-P1	GTCATCCATCATGACGCAAAG	CTGGTGATTGGACAGTTTGATG	ChIP-qPCR
ANAC081-P2	AGAATTGTCATGATGGGTTGTAAAG	GTCATTGCTTGCGTCACTTAAAC	ChIP-qPCR
ANAC087-P1	GAGAGACGCTAGTTTCACACC	TTAGCTCAAACTTAGTCATTG	ChIP-qPCR
ANAC087-P2	TATCAATGACTAAGTTTGAGC	GAAAGATACGTACGCTCCAAG	ChIP-qPCR
At3g12910-P1	GAAATCCGATATGCCGATCTTTG	CAGCTACGGGATGGTTCATAA	ChIP-qPCR
At3g12910-P2	CAGTCCTCTCCTTAGCGTTTTC	GAGTCTTTTCGCATCTATACG	ChIP-qPCR
TA3	CTGCGTGGAAGTCTGTCAAA	CTATGCCACAGGGCAGTTTT	ChIP-qPCR

Supplementary Datasets

Dataset S1. Differentially expressed *NAC*s at four stages. For each stage (14, 18, 22, or 26 days of leaf age), the list of target NACs significantly (FDR ≤ 0.1; Methods) up- or down-regulated in 49 *nac* mutants, compared to wild type, at the stage is shown with their $\log_2$-fold-changes and FDRs.

See the attached excel file named “Dataset S1.xlsx”.

Dataset S2. DEGs in mutants of the NAC troika, compared to wild type, at a pre-senescent stage. For each DEG, TAIR ID and gene name and description in TAIR database are shown together with $\log_2$-fold-changes and the combined *P* values (*Materials and Methods*) in the three comparisons: 1) *anac017* vs. wild type (*anac017*/Col); 2) *anac082* vs. wild type (*anac082*/Col); and 3) *anac090* vs. wild type (*anac090*/Col). The values were shown only for the comparisons with significant combined *P* values.

See the attached excel file named “Dataset S2.xlsx”.

Dataset S3. GOBPs enriched by genes in G1-8. Eight tables for the GOBPs enriched by G1-8, respectively, are provided (G1 to G8 labeled tables). In the individual tables, for each GOBP, the GO term ID and description are shown together with the number of genes annotated with the GOBP (Count) and the enrichment *P* value for the GOBP. The GOBPs shown in Fig. 3*B* are highlighted in yellow backgrounds.

See the attached excel file named “Dataset S3.xlsx”.

Dataset S4. Genes that were more strongly regulated by the individual hub NACs. Six tables for the genes in P1-6 are provided (P1 to P6 labeled tables). In the individual tables, for each gene, TAIR ID and gene name and description in TAIR database are shown together with $\log_2$-fold-changes and the combined *P* values (Methods) in the indicated comparisons: for P1 and P4, *anac017* vs. *anac082* (*anac017*/*anac082*) and *anac017* vs. *anac090* (*anac017*/*anac090*); for P2 and P5, *anac082* vs. *anac017* (*anac082*/*anac017*) and *anac082* vs. *anac090* (*anac082*/*anac090*); and for P3 and P6, *anac090* vs. *anac017* (*anac090*/*anac017*) and *anac090* vs. *anac082* (*anac090*/*anac082*). The values were shown only for the comparisons with significant combined *P* values.

See the attached excel file named “Dataset S4”.

Dataset S5. GOBPs enriched by genes in P1-6. Six tables for the GOBPs enriched by P1-6, respectively, are provided (P1 to P6 labeled tables). In the individual tables, for each GOBP, the GO term ID and description are shown together with the number of genes annotated with the GOBP (Count) and the enrichment *P* value for the GOBP. The GOBPs shown in Fig. 4*B* are highlighted in yellow backgrounds.

See the attached excel file named “Dataset S5.xlsx”.

Dataset S6. Information of interactions used for building the network model. For each

interaction used in Supplementary Fig. 8*B*, the interaction type (protein-DNA/protein interaction, activation, induction, reduction, synthesis, and functional association), the source of interaction (interactome database or literature curation), and the description for the interaction in the literature are shown together with the reference. An arrow denotes the regulatory direction between the connected components.

See the attached excel file named “Dataset S6.xlsx”.

Supplementary References

1. Jin J, Tian F, Yang DC, Meng YQ, Kong L, Luo J, Gao G (2016) PlantTFDB 4.0: toward a central hub for transcription factors and regulatory interactions in plants. *Nucleic Acids Res*. 45:D1040-1045.
2. Woo HR, Koo HJ, Kim J, Jeong H, Yang JO, Lee IH, Jun JH, Choi SH, Park SJ, Kang B, Kim YW, Phee BK, Kim JH, Seo C, Park C, Kim SC, Park S, Lee B, Lee S, Hwang D, Nam HG, Lim PO (2016) Programming of Plant Leaf Senescence with Temporal and Inter-Organellar Coordination of Transcriptome in *Arabidopsis*. *Plant Physiol* 171:452-467.
3. Brumbaugh CD, Kim HJ, Giovacchini M, Pourmand N (2011) NanoStriDE: normalization and differential expression analysis of NanoString nCounter data. *BMC Bioinformatics* 12:479.
4. Chae S, Ahn BY, Byun K, Cho YM, Yu MH, Lee B, Hwang D, Park KS (2013) A systems approach for decoding mitochondrial retrograde signaling pathways. *Sci Signal* 6:rs4.
5. Kim JH, Woo HR, Kim J, Lim PO, Lee IC, Choi SH, Hwang D, Nam HG (2009) Trifurcate feed-forward regulation of age-dependent cell death involving miR164 in *Arabidopsis*. *Science* 323:1053-1057.
6. Oh SA, Lee SY, Chung IK, Lee CH, Nam HG (1996) A senescence-associated gene of *Arabidopsis thaliana* is distinctively regulated during natural and artificially induced leaf senescence. *Plant Mol Biol* 30:739-754.
7. Oh SA, Park JH, Lee GI, Paek KH, Park SK, Nam HG (1997) Identification of three genetic loci controlling leaf senescence in *Arabidopsis thaliana*. *Plant J* 12:527-535.

8. Lichtenthaler HK (1987) Chlorophylls and Carotenoids - Pigments of Photosynthetic Biomembranes. *Methods Enzymol.* 148:350-382.

9. Uknes S, Winter AM, Delaney T, Vernooij B, Morse A, Friedrich L, Nye G, Potter S, Ward E, Ryals J (1993) Biological Induction of Systemic Acquired-Resistance in *Arabidopsis*. *Mol. Plant-Microbe Interact.* 6:692-698.

10. Lamesch P, Berardini TZ, Li D, Swarbreck D, Wilks C, Sasidharan R, Muller R, Dreher K, Alexander DL, Garcia-Hernandez M, Karthikeyan AS, Lee CH, Nelson WD, Ploetz L, Singh S, Wensel A, Huala E (2012) The Arabidopsis Information Resource (TAIR): improved gene annotation and new tools. *Nucleic Acids Res* 40:D1202-1210.

11. Trapnell C, Pachter L, Salzberg SL (2009) TopHat: discovering splice junctions with RNA-Seq. *Bioinformatics* 25:1105-1111.

12. Trapnell C, Williams BA, Pertea G, Mortazavi A, Kwan G, van Baren MJ, Salzberg SL, Wold BJ, Pachter L (2010) Transcript assembly and quantification by RNA-Seq reveals unannotated transcripts and isoform switching during cell differentiation. *Nat Biotechnol* 28:511-515.

13. Graveley BR, Brooks AN, Carlson JW, Duff MO, Landolin JM, Yang L, Artieri CG, van Baren MJ, Boley N, Booth BW, Brown JB, Cherbas L, Davis CA, Dobin A, Li R, Lin W, Malone JH, Mattiuzzo NR, Miller D, Sturgill D, Tuch BB, Zaleski C, Zhang D, Blanchette M, Dudoit S, Eads B, Green RE, Hammonds A, Jiang L, Kapranov P, Langton L, Perrimon N, Sandler JE, Wan KH, Willingham A, Zhang Y, Zou Y, Andrews J, Bickel PJ, Brenner SE, Brent MR, Cherbas P, Gingeras TR, Hoskins RA, Kaufman TC, Oliver B, Celniker SE (2011) The developmental transcriptome of *Drosophila melanogaster*. *Nature* 471:473-479.

14. Bolstad BM, Irizarry RA, Astrand M, Speed TP (2003) A comparison of normalization methods for high density oligonucleotide array data based on variance and bias. *Bioinformatics* 19:185-193.

15. Lee HJ, Suk JE, Patrick C, Bae EJ, Cho JH, Rho S, Hwang D, Masliah E, Lee SJ (2010) Direct transfer of alpha-synuclein from neuron to astroglia causes inflammatory responses in synucleinopathies. *J Biol Chem* 285:9262-9272.

16. Hwang D, Rust AG, Ramsey S, Smith JJ, Leslie DM, Weston AD, de Atauri P, Aitchison JD, Hood L, Siegel AF, Bolouri H (2005) A data integration methodology for systems biology. *Proc Natl Acad Sci U S A* 102:17296-17301.

17. Huang da W, Sherman BT, Lempicki RA (2009) Systematic and integrative analysis of large gene lists using DAVID bioinformatics resources. *Nat Protoc* 4:44-57.

18. Mueller LN, Rinner O, Schmidt A, Letarte S, Bodenmiller B, Brusniak MY, Vitek O, Aebersold R, Muller M (2007) SuperHirn - a novel tool for high resolution LC-MS-based peptide/protein profiling. *Proteomics* 7:3470-3480.

19. Raskin I, Turner IM, Melander WR (1989) Regulation of heat production in the inflorescences of an Arum lily by endogenous salicylic acid. *Proc Natl Acad Sci U S A* 86:2214-2218.

20. Riehl Koch J, Scherzer AJ, Eshita SM, Davis KR (1998) Ozone sensitivity in hybrid poplar is correlated with a lack of defense-gene activation. *Plant Physiol* 118:1243-1252.

21. Zhu Y, Dong AW, Shen WH (2012) Histone variants and chromatin assembly in plant abiotic stress responses. *Biochim. Biophys. Acta* 1819:343-348.

22. Hwang I, Sheen J (2001) Two-component circuitry in *Arabidopsis* cytokinin signal transduction. *Nature* 413:383-389.

23. Kim J, Somers DE (2010) Rapid assessment of gene function in the circadian clock using artificial microRNA in *Arabidopsis* mesophyll protoplasts. *Plant Physiol* 154:611-621.

24. Hellens RP, Allan AC, Friel EN, Bolitho K, Grafton K, Templeton MD, Karunairetnam S, Gleave AP, Laing WA (2005) Transient expression vectors for functional genomics, quantification of promoter activity and RNA silencing in plants. *Plant Methods* 1:13.

25. Chow CN, Zheng HQ, Wu NY, Chien CH, Huang HD, Lee TY, Chiang-Hsieh YF, Hou PF, Yang TY, Chang WC (2016) PlantPAN 2.0: an update of plant promoter analysis navigator for reconstructing transcriptional regulatory networks in plants. *Nucleic Acids Res* 44:D1154-1160.